Concurrent field enhancement and high transmission of THz radiation in nanoslit arrays

Mostafa Shalaby, Hannes Merbold, Marco Peccianti, Luca Razzari, Gargi Sharma, Tsuneyuki Ozaki, Roberto Morandotti, Thomas Feurer, Anja Weber, Laura Heyderman, Bruce Patterson, and Hans Sigg

Citation: Applied Physics Letters **99**, 041110 (2011); doi: 10.1063/1.3617476
View online: http://dx.doi.org/10.1063/1.3617476
View Table of Contents: http://scitation.aip.org/content/aip/journal/apl/99/4?ver=pdfcov
Published by the AIP Publishing

Articles you may be interested in

Resonance enhancement of difference-frequency generation through localized surface plasmon excitation
Appl. Phys. Lett. **102**, 203101 (2013); 10.1063/1.4807169

Resonant transmission of light through ZnO nanowaveguides in a silver film
Appl. Phys. Lett. **101**, 081113 (2012); 10.1063/1.4747718

Terahertz propagation properties of free-standing woven-steel-mesh metamaterials: Pass-bands and signatures of abnormal group velocities
J. Appl. Phys. **110**, 064902 (2011); 10.1063/1.3638445

Midinfrared filters based on extraordinary optical transmission through subwavelength structured gold films
J. Appl. Phys. **106**, 124313 (2009); 10.1063/1.3272716

Enhanced microwave transmission through quasicrystal hole arrays
Appl. Phys. Lett. **91**, 081503 (2007); 10.1063/1.2773763

This article is copyrighted as indicated in the article. Reuse of AIP content is subject to the terms at: http://scitation.aip.org/termsconditions. Downloaded to IP: 192.33.101.210 On: Tue, 01 Apr 2014 13:26:01

Concurrent field enhancement and high transmission of THz radiation in nanoslit arrays

Mostafa Shalaby,[1,a)] Hannes Merbold,[2,b)] Marco Peccianti,[1,c)] Luca Razzari,[1,d)] Gargi Sharma,[1] Tsuneyuki Ozaki,[1] Roberto Morandotti,[1] Thomas Feurer,[2] Anja Weber,[3] Laura Heyderman,[3] Bruce Patterson,[4] and Hans Sigg[3]
[1]*INRS-EMT, Varennes, Quebec J3X 1S2, Canada*
[2]*IAP, University of Bern, Sidlerstrasse 5, Bern 3012, Switzerland*
[3]*LMN, Paul Scherrer Institut, Villigen 5232, Switzerland*
[4]*SwissFEL, Paul Scherrer Institut, Villigen 5232, Switzerland*

(Received 12 April 2011; accepted 7 July 2011; published online 28 July 2011)

We experimentally and numerically investigate the transmission of THz radiation through uniform nanoslit arrays. These structures are capable of inducing plasmon-mediated field enhancement while concurrently providing high field transmission. Combined with intense THz radiation, estimated field strengths as high as 26 MV/cm are obtained in the near-field regime which will facilitate nonlinear THz experiments. © *2011 American Institute of Physics*. [doi:10.1063/1.3617476]

Since the report of high optical transmission in subwavelength hole arrays,[1] transmission and field enhancement properties of electro-magnetic waves in subwavelength metallic apertures have drawn much interest.[2] In the THz regime, field enhancement is of importance due to the present technological limitations in the peak fields obtainable from current THz sources[3] which limits the realization of nonlinear THz experiments.[4–6] Recently, Seo *et al.*[7] reported a field enhancement factor F approaching 780 at 0.1 THz using a single 70 nm wide slit etched in a thin gold film. A single slit can be depicted as a nanocapacitor loaded with the charge collected by the surrounding metal surface. When THz radiation impinges on the metal sheet, light-induced current creates transients of charge imbalance across the gap. This imbalance, in turn, leads to a field enhancement inside the gap that scales with the incident wavelength.[7] Despite the high field enhancement obtainable in single slits, such structures tend to suffer from a low field transmission T, which could in principle be increased by arranging the slits into arrays.[8,9] However, the net charge imbalance depends on the current induced within a finite collection area around the gap. Hence, as the spacing between the slits decreases, the collected charge per slit, and, therefore, the overall field enhancement factor, decreases. A compromise can be found to obtain reasonable values of F and T by optimizing the array parameters. In this work, we design and experimentally demonstrate 1D arrays of nanoslits featuring high T while preserving high F in the frequency range of 0.2–2.7 THz.

Figure 1(a) shows a schematic of a 1D nanoslit array patterned in a thin metal film. Throughout this work, we assume that the incident electromagnetic wave is polarized perpendicular to the slits' long axis as indicated. For an infinitely long 1D array, the structural parameters for adjusting F and T are the slit height h, the width a, and the periodicity d. Decreasing h, in general, enhances F as it increases the charge carrier density in the gap region. However, as h becomes smaller than the skin depth, the gold film starts to be transparent to the THz radiation, reducing the amount of field energy effectively contributing to the enhancement. Hence, we chose $h = 60$ nm, which is comparable to the skin depth of gold at 1 THz (70 nm). The field enhancement has been shown to increase as a decreases, with the lower limit determined by the charge-screening length ($\lesssim$1 nm).[7] In practice, a is limited by the smallest feature size that can be achieved in the fabrication process, here approximately 40 nm. The periodicity d is, therefore, the main design parameter that can be modified. Sophisticated numerical simulations, which also give details on the local charge distribution, have been performed using frequency- and time-dependent finite element methods (FEM) in two spatial dimensions as described in Ref. 10. The frequency-dependent simulations yield the transmission $T(\nu) = E_{\text{out}}(\nu)/E_{\text{inc}}(\nu)$ as well as the field enhancement factor $F(\nu) = E_{\text{gap}}(\nu)/E_{\text{inc}}(\nu)$, where $E_{\text{gap}}(\nu)$ denotes the absolute amplitude of the electric field in mid-gap, and $E_{\text{inc}}(\nu)$ and $E_{\text{out}}(\nu)$, the amplitude of the incident and transmitted field, respectively. The time-dependent simulations yield the spatiotemporal field distribution and, more importantly, they confirm that the in-gap field transient is reproduced by the waveform sampled in the far-field, information that is important to estimate the absolute in-gap field strengths from the measured far-field traces.

Figures 2 show the simulated transmission and field enhancement factor for a free standing 1D array as the

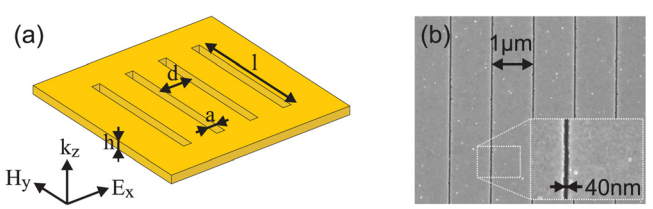

FIG. 1. (Color online) (a) Schematic illustration of a 1D nanoslit array. (b) Scanning electron microscope image with the inset showing a zoomed-in image of one of the slits.

[a)]Electronic mail: shalaby@emt.inrs.ca.
[b)]Electronic mail: hannes.merbold@iap.unibe.ch.
[c)]Also at IPCF-CNR, Sapienza University, P.A. Moro 8, Rome 00185, Italy.
[d)]Also at Italian Institute of Technology, Via Morego 30, Genova 16163, Italy.

 © 2011 American Institute of Physics

This article is copyrighted as indicated in the article. Reuse of AIP content is subject to the terms at: http://scitation.aip.org/termsconditions. Downloaded to IP: 192.33.101.210 On: Tue, 01 Apr 2014 13:26:01

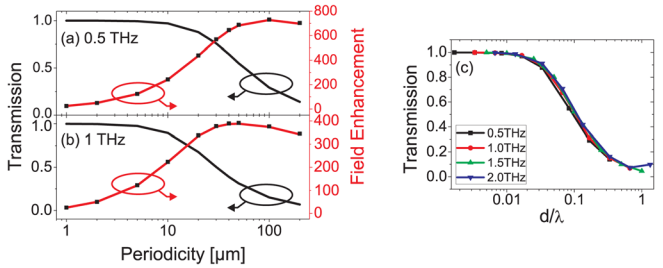

FIG. 2. (Color online) Field enhancement factor F (red curve) and transmission T (black curve) for varying periodicity d at (a) 0.5 THz and (b) 1 THz. The black squares represent $F = T/\beta$. (c) Transmission versus d/λ for four different frequencies.

periodicity is varied for a frequency of 0.5 THz and 1 THz, respectively. As demonstrated in Ref. 7, there is no penetration of the electric field of the average Pointing vector within the side of the slit even for a metal with finite conductivity. The in-gap field is fully scattered to the far-field[7] and we find

$$F(\nu) = T(\nu)/\beta, \tag{1}$$

where $\beta = a/d$ is the aperture coverage. This is shown by the black squares corresponding to F calculated from the far-field transmission, which reproduces the field enhancement sampled in mid-gap. For a small periodicity, the transmission values are close to unity and the field enhancement factors are small. This behavior reverses as the slit spacing increases. The field enhancement relies on a finite collection distance f_l, oriented normally to the slits' long axis, where the incident field energy is gathered and subsequently funneled through the slit aperture.[11] If the spacing between the slits is less than f_l, the slits share the collected charges and the field enhancement decreases. A high transmission, however, relies on designing dense slit structures. Therefore, a compromise should be found between T and F. While this general behavior is observed for all frequencies, the details are frequency-dependent, and consequently such a compromise has to be optimized in the spectral range of interest. As shown in Fig. 2(c), the transmission versus the ratio d/λ is independent of frequency which also shows that the funneling is a purely geometric effect. We find that a transmission attenuated by less than 3 dB demands $d \leq \lambda/15$ where the corresponding field enhancement can again be determined using Eq. (1). These results allow one to choose the optimum periodicity for the realization of nonlinear THz experiments. For a second order nonlinear process, for example, the quantity to be optimized is F^2/d since such a process exhibits a quadratic dependence on the induced field strength and scales linearly with the overall size of the high field strength volume.[10] Using Eq. (1), the quantity F^2/d is seen to be directly proportional to $F\,T$ so that, in Figs. 2, the ideal periodicity is approximately given by the crossing point between the red and the black curves. Considering the whole spectral range between 0.2 THz and 2.7 THz, we find that a high field enhancement, comparable to the single slit case, is maintained for slit spacings of $d \gtrsim 50\mu$m.

Based on the above consideration and on the fabrication constraints, we prepared two arrays of 40 nm wide slits, placed at 1 μm and 100 μm intervals, in a 60 nm thick Au film. As the sample substrate, we used a 500 μm thick high resistivity silicon wafer. Our sample was realized using electron-beam lithography, combined with evaporation of a gold film on a 5 nm thick Cr adhesion layer and subsequent lift-off. This process yields narrow rectangular apertures (2 mm $\times$ 40 nm) with an aspect ratio l/a of 50 000. The slits were patterned within an area of 2 mm $\times$ 2 mm, which is larger than our THz spot size (1.2 mm), thus justifying the assumption of infinitely long slits and an infinite array extension. A scanning electron microscope image of part of a nanoslit array and a zoomed-in image of one of the slits is shown in Fig. 1(b).

The spatiotemporal electric field distribution behind the nanoslit arrays was investigated with our THz polaritonics platform. An in-depth description of this technique can be found in Ref. 12. We employ an experimental geometry where the slit array on the Si substrate is sandwiched between two lithium niobate (LN) crystals.[13,14] THz waves are generated in the first crystal, propagate through the sample, and are visualized in the second crystal. Snapshots of the waveforms detected in the probe crystal are shown in Figs. 3 where the white arrows mark the propagation direction. The reference THz wave, i.e., no slit array present, is shown in Fig. 3(a). When the nanoslit array with 1 μm slit spacing is inserted (marked by the dashed white line in Fig. 3(b)), almost no change in waveform is observed and the transmission is close to one although the slit coverage β is only 1/25. Even for the 100 μm periodicity sample ($\beta = 1/2500$), the transmission is still rather high and the emergence of additional features is observed, most noticeably the interference pattern trailing the zeroth order waveform as marked by the blue curves. This interference pattern, which results from the coherent superposition of the fields transmitted through the individual slits,[14] can best be seen in a video showing the temporal evolution of the measured waveform (available in the supporting online material). Figure 3(d) shows a time dependent simulation of the employed sandwich geometry. The waveform transmitted into the right LN crystal reproduces all details observed in the measurement, i.e., the interference features as well as the weak replica following the main THz

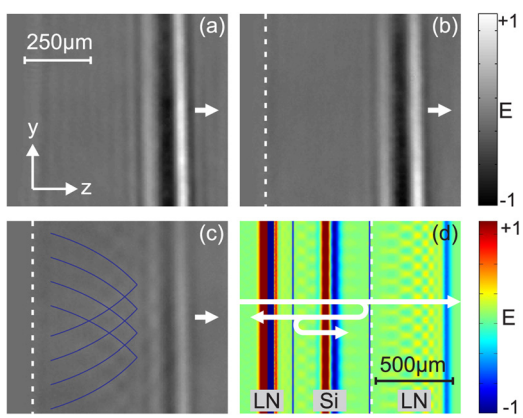

FIG. 3. (Color online) Snapshots of the spatial field distribution measured approximately 10 ps after the THz pulse has passed through a substrate (a) without slits, and with slits having (b) 1 μm, and (c) 100 μm spacing (enhanced online, Video 1) [URL: http://dx.doi.org/10.1063/1.3617476.1]. The images are plotted on the same absolute gray scale. (d) Simulation corresponding to (c) showing the entire sandwich geometry (enhanced online, Video 2) [URL: http://dx.doi.org/10.1063/1.3617476.2].

This article is copyrighted as indicated in the article. Reuse of AIP content is subject to the terms at: http://scitation.aip.org/termsconditions. Downloaded to IP: 192.33.101.210 On: Tue, 01 Apr 2014 13:26:01

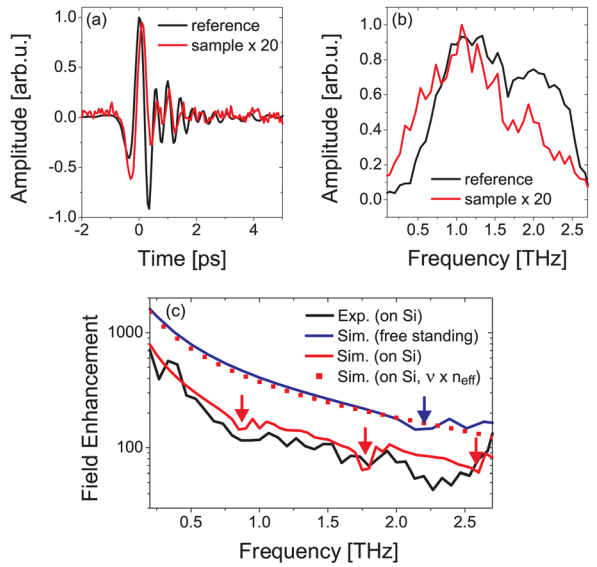

FIG. 4. (Color online) (a) Time profile of THz pulses transmitted through an unstructured Si substrate and the $d = 100$ μm slit array. (b) Corresponding spectra. (c) Simulated enhancement factor for a freestanding $d = 100$ μm array, the slit array on substrate, and the field enhancement obtained from the measurement. The arrows mark the spectral modulations related to grating modes.

waveform, which stems from multiple reflections in the silicon substrate. This behavior is again most illustrative in a video showing the temporal evolution of the simulated waveform (available in the supporting online material).

In order to analyze the transmission and the field enhancement factor more quantitatively, we also performed transmission measurements using THz time domain spectroscopy.[15] Here, we focus on the slit array with 100 μm periodicity due to its larger field enhancement. The time profiles and spectral contents of the reference (pure substrate) and sample pulses are shown in Figs. 4, respectively. By simply dividing the spectra, we obtain the transmission $T(\nu)$ from which we calculate the field enhancement using Eq. (1). In Fig. 4(c), the experimentally obtained field enhancement factor in the spectral range 0.2–2.7 THz, along with FEM simulations for the freestanding slit array and the slit array on substrate are shown. Good agreement is obtained between the measurement and the simulation for the slits on the Si substrate. The reduced field enhancement, as compared to the freestanding case, is explained by the slit array responding to an effectively smaller wavelength $\lambda_{\text{eff}} = \lambda_0/n_{\text{eff}}$, where λ_0 denotes the free space wavelength and $n_{\text{eff}} = \sqrt{(n_{\text{Si}}^2 + n_{\text{Air}}^2)/2}$. As indicated by the red squares, the freestanding case is reproduced by the on-substrate case if the frequency axis is scaled by n_{eff}. Note that this wavelength scaling has to be taken into account when optimizing the array's periodicity for the investigation of THz nonlinearities. The arrows in Fig. 4(c) mark irregularities that are assigned to grating modes where the slit array diffracts the incident radiation into the sample plane.[16] In the Si substrate, the wavelength decreases according to λ_0/n_{Si} so that, compared to a freestanding slit array, the grating modes are shifted to smaller frequencies. At a frequency of 0.2 THz, we measure a field enhancement factor of $F = 760$ corresponding to 30% transmission despite the aperture coverage being as low as $\beta = 1/2500$.

The most intense THz pulses used here, with a peak electric field of about 200 kV/cm, were generated by means of optical rectification of 70 mJ laser pulses in a large aperture (3 in.) ZnTe crystal.[17] For the THz transient of such a pulse transmitted through the slit array, we measure a peak field transmission of 5.2% (10.4 kV/cm) which, together with the aperture coverage, yields a estimated field strength inside the slit of $E = 26$ MV/cm.

In conclusion, we have investigated 1D arrays of nanoslits with the goal of achieving a good compromise between the enhancement factor and the transmission in the 0.2–2.7 THz frequency range. We have demonstrated experimentally that an array of 40 nm wide slits with 100 μm periodicity shows a peak near-field enhancement factor of 760 at 0.2 THz, corresponding to 30% transmission. Combined with an intense source, THz field strengths as high as 26 MV/cm are obtained. These intense and relatively broadband pulses open the way to nonlinear THz experiments.

M.S. would like to thank Ibraheem Elnaib (INRS-EMT) for helpful discussions. This work is supported by the FQRNT, the NSERC, and the SNSF (project 200020-119934 and NCCR-MUST). M.S. and M.P. wish to acknowledge a FQRNT MELS scholarship and a Marie Curie Outgoing International Fellowship (Contract No. PIOF-GA-2008-221262), respectively.

[1]T. Ebbesen, H. Lezec, H. Ghaemi, T. Thio, and P. Wolff, Nature **391**, 667 (1998).
[2]F. J. Garcia-Vidal, L. Martin-Moreno, T. W. Ebbesen, and L. Kuipers, Rev. Mod. Phys. **82**, 729 (2010).
[3]A. G. Stepanov, L. Bonacina, S. V. Chekalin, and J.-P. Wolf, Opt. Lett. **33**, 2497 (2008).
[4]T. Qi, Y.-H. Shin, K.-L. Yeh, K. A. Nelson, and A. M. Rappe, Phys. Rev. Lett. **102**, 247603 (2009).
[5]T. Kampfrath, A. Sell, G. Klatt, A. Pashkin, S. Mahrlein, T. Dekorsy, M. Wolf, M. Fiebig, A. Leitenstorfer, and R. Huber, Nat. Photonics **5**, 31 (2011).
[6]L. Razzari, F. H. Su, G. Sharma, F. Blanchard, A. Ayesheshim, H.-C. Bandulet, R. Morandotti, J.-C. Kieffer, T. Ozaki, M. Reid, and F. A. Hegmann, Phys. Rev. B **79**, 193204 (2009).
[7]M. Seo, H. Park, S. Koo, D. Park, J. Kang, O. Suwal, S. Choi, P. Planken, G. Park, N. Park, Q. Park, and D. Kim, Nat. Photonics **3**, 152 (2009).
[8]J. H. Kang, Q.-H. Park, J. W. Lee, M. A. Seo, and D. S. Kim, J. Kor. Phys. Soc. **49**, 881 (2006).
[9]H. Park, Y. Park, H. Kim, J. Kyoung, M. Seo, D. Park, Y. Ahn, K. Ahn, and D. Kim, Appl. Phys. Lett. **96**, 121106 (2010).
[10]H. Merbold, A. Bitzer, and T. Feurer, Opt. Express **19**, 7262 (2011).
[11]D. Kim, M. Seo, H. Park, J. Kyoung, J. Lee, O. Suwal, and S. Choi, Proc. SPIE **7214**, 72140H (2009).
[12]T. Feurer, N. S. Stoyanov, D. W. Ward, J. C. Vaughan, E. R. Satz, and K. A. Nelson, Annu. Rev. Mater. Res. **37**, 317 (2007).
[13]H. Merbold and T. Feurer, J. Appl. Phys. **107**, 033504 (2010).
[14]H. Merbold, A. Bitzer, F. Enderli, and T. Feurer, J. Infrared Millim. Waves **32**, 570 (2011).
[15]M. van Exter, C. Fattinger, and D. Grischkowsky, Opt. Lett. **14**, 1128 (1989).
[16]A. Bitzer, J. Wallauer, H. Merbold, H. Helm, T. Feurer, and M. Walther, Opt. Express **17**, 22108 (2009).
[17]F. Blanchard, L. Razzari, H. Bandulet, G. Sharma, R. Morandotti, J. Kieffer, T. Ozaki, M. Reid, H. Tiedje, H. Haugen, and F. Hegmann, Opt. Express **15**, 13212 (2007).

This article is copyrighted as indicated in the article. Reuse of AIP content is subject to the terms at: http://scitation.aip.org/termsconditions. Downloaded to IP: 192.33.101.210 On: Tue, 01 Apr 2014 13:26:01